

Multiscale correlations and conditional averages in numerical turbulence

Siegfried Grossmann,^{1,*} Detlef Lohse,^{2,†} and Achim Reeh^{1,‡}

¹*Fachbereich Physik der Philipps-Universität, Renthof 6, D-35032 Marburg, Germany*

²*Department of Applied Physics and J. M. Burgers Centre for Fluid Dynamics, University of Twente, P.O. Box 217, 7500 AE Enschede, The Netherlands*

(Received 14 May 1999; revised manuscript received 15 November 1999)

The equations of motion for the n th order velocity differences raise the interest in correlation functions containing both large and small scales simultaneously. We consider the scaling of such objects and also their conditional average representation with emphasis on the question of whether they behave differently in the inertial or the viscous subranges. The turbulent flow data are obtained by Navier-Stokes solutions on a 60^3 grid with periodic boundary conditions and $\text{Re}_\lambda = 70$. Our results complement previous high Re data analysis based on measured data [A. L. Fairhall, V. S. L'vov, and I. Procaccia, *Europhys. Lett* **43**, 277 (1998)] whose preference were the larger scales, and the analysis of both experimental and synthetic turbulence data by [R. Benzi and co-workers, *Phys. Rev. Lett.* **80**, 3244 (1998); *Phys. Fluids* **11**, 2215 (1999)]. The inertial range fusion rule is confirmed and insight is obtained for the conditional averages (the local dissipation rate conditioned on the velocity fluctuations).

PACS number(s): 47.27.-i

To analyze the structure of turbulent flow fields Lagrangean longitudinal n th order structure functions $S_n(R) = \langle v^n(R) \rangle$ are of utmost importance. Here $v(x, R; t) = [\mathbf{u}(x + \mathbf{R}, t) - \mathbf{u}(x, t)] \cdot \mathbf{R}/R$ denotes the longitudinal velocity difference on scale R . The equation of motion (cf. [1,2]) in the case of statistically stationary turbulence

$$\partial_t S_n(R, t) = 0 = -n\mathcal{D}_n(R, t) + \nu n J_n(R, t), \quad (1)$$

introduces correlation functions of another type, containing local gradient and curvature in addition to the scale R . The $(\mathbf{u} \cdot \nabla)\mathbf{u}$ nonlinearity in the Navier-Stokes equation gives rise to $\mathcal{D}_n(R, t)$ (which needs no further specification here because we do not consider it in what follows) and the viscous term $\nu \Delta \mathbf{u}$ leads to $J_n = \langle \Delta u v^{n-1}(R) \rangle$. The Laplacean probes the *local* behavior, while R is in the *inertial* range. This two-scale character of J_n becomes explicit if the local curvature Δu is approximated by finite differences, $\Delta_r u(x) = [u(x+r) - 2u(x) + u(x-r)]/r^2$. The necessity for this discretization arises both in numerical turbulence and in the analysis of measured flow signals. It motivates to study the following more general objects:

$$J_n(r, R) = r^{-2} \langle [u(x+r) - 2u(x) + u(x-r)] \times [u(x+R) - u(x)]^{n-1} \rangle. \quad (2)$$

Here $r \ll R$ is assumed, and r (instead of $r \rightarrow 0$) is allowed to vary in the viscous as well as in the inertial subranges VSR and ISR. In particular r may be below or above η_n , where η_n denotes the transition scale between VSR and ISR in an n th order correlation function. It is these J_n on which we concentrate in this note.

The two-scale correlators J_n are of interest to check the validity of the so-called fusion rules [3,4]. These describe the proper factorization of the general n th order correlation functions

$$\mathcal{F}_n(\mathbf{x}_1, \mathbf{x}'_1; \mathbf{x}_2, \mathbf{x}'_2; \dots; \mathbf{x}_n, \mathbf{x}'_n) := \langle \mathbf{v}(\mathbf{x}_1, \mathbf{x}'_1) \cdots \mathbf{v}(\mathbf{x}_n, \mathbf{x}'_n) \rangle,$$

if a subgroup of p pairs $\mathbf{x}_i - \mathbf{x}'_i$ becomes much smaller, “fuses,” than the remaining $n-p$ pairs, $1 < p < n$. Let the fusing pairs have scale r , the nonfusing ones scale R . If $r \ll R$, the r eddies are supposed to be statistically independent from the large scale motion R and vice versa. This might naively suggest to factorize $\mathcal{F}_n(r, R) \approx \mathcal{F}_p(r) \mathcal{F}_{n-p}(R)$. But this turns out as too naive, because it contradicts the scaling of the n th order correlation functions under dilation of distances, unless the scaling exponents ζ_n are linear in n . Namely, define the scaling exponents ζ_n by

$$\mathcal{F}_n(\lambda r, \lambda R) = \lambda^{\zeta_n} \mathcal{F}_n(r, R). \quad (3)$$

The naive factorization immediately leads to $\zeta_n = \zeta_p + \zeta_{n-p}$. Thus a relation between the scaling exponents obtains which implies $\zeta_n = \zeta_1 n$, meaning that only *one* non-trivial scaling exponent exists (“monoscaling”). To allow for the possibility of multiscaling, equivalent to nonlinear n dependence of the scaling exponents, the naive factorization ansatz has to be avoided, because it jeopardizes multiscaling by assumption.

A more general factorization of the multiscale correlation functions $\mathcal{F}_n(r, R)$, denoted as “fusion rule” by L'vov and Procaccia [3,4], starts with the decomposition $\mathcal{F}_n(r, R) = \mathcal{F}_p(r) \tilde{\mathcal{F}}_{p, n-p}(r, R)$, the second factor being defined by this equation. Here it is assumed that the small r eddies move in the field of the larger, slower R eddies as they would do also without the large scale motion, and are described therefore by the p correlator of the p smaller r eddies $v_i(r)$. The statistical independence of the small and the large scales is expressed by skipping the r dependence of the large scale eddy

*Electronic address: grossmann_s@physik.uni-marburg.de

†Electronic address: lohse@tn.utwente.nl

‡Electronic address: reeh@mailier.uni-marburg.de

correlation $\tilde{\mathcal{F}}_{p,n-p}(r,R)$. But even if $\tilde{\mathcal{F}}_{p,n-p}(R)$ is assumed to be independent of the small scale r , it may remember its origin from an n -point correlator. Performing the dilation transformation of the product $\mathcal{F}_p \tilde{\mathcal{F}}_{p,n-p}$ of correlation functions with λ leads to

$$\tilde{\mathcal{F}}_{p,n-p}(\lambda R) = \lambda^{\xi_n - \xi_p} \tilde{\mathcal{F}}_{p,n-p}(R), \quad (4)$$

provided r and R are in the same, inertial scaling range. The scaling behavior (4) is obtained if $\tilde{\mathcal{F}}_{p,n-p}(R)$ is expressed as the ratio of an n th and a p th order correlation function, i.e., $\tilde{\mathcal{F}}_{p,n-p}(R) \propto S_n(R)/S_p(R)$, and therefore the scaling invariant factorization reads

$$\mathcal{F}_n(r,R) \sim S_p(r) S_n(R)/S_p(R). \quad (5)$$

The symbol \sim is to be understood as ‘‘scaling wise.’’ Clearly both the left-hand side (LHS) and the RHS rescale

$$J_n(r,R) = r^{-2} \langle [2u^2(x) - u(x+r)u(x) - u(x-r)u(x)] v^{n-2}(R) \rangle.$$

Because of spatial translational invariance this can be rearranged to give

$$J_n(r,R) = r^{-2} \langle v^2(r) v^{n-2}(R) \rangle, \quad r \ll R. \quad (6)$$

The objects J_n are now in the form of a two-scale correlation function to which the factorization (‘‘fusion’’) rules can be applied and their validity be checked. We do this for r in the ISR according to Eq. (5) and later on also for r in the VSR.

Let us first consider the fusion rule for $\eta_n \ll r \ll R \ll L$, both scales being in the ISR (L being the outer scale). It says by Eq. (5) that

$$J_n(r,R) = C_n r^{-2} S_2(r) S_n(R)/S_2(R). \quad (7)$$

All these correlation functions S_n and S_2 can easily be computed from a numerical turbulent flow solution of the Navier-Stokes equation, the $J_n(r,R)$ according to their defining formula (2), and the S_n according to their definition $\langle v^n \rangle$. If n is odd it makes a difference if v^n or $|v|^n = (\sqrt{v^2})^n$ is used, see Ref. [5]; we distinguish these cases as S_n and S_n^* . Typical averaging times are about 100 large eddy turnovers. Forcing is on the largest scale. The periodicity length of the box then is $2\pi L$. Lengths are nondimensionalized with this length L . Time is nondimensionalized with $(L^2/\epsilon)^{1/3}$. Thus the nondimensional energy dissipation rate per mass becomes $\epsilon = 1$. The (dimensionless) velocities are always divided by the rms velocity, which in our flow turns out to be $u_{\text{rms}} = 1.40$. The viscous length scale for the second order correlations is $\eta_2 \equiv \eta = (\nu^3/\epsilon)^{1/4} = 9 \times 10^{-3} L$. For the averaging the vectors \mathbf{r} and \mathbf{R} are chosen as $r(1,0,0)$ and $R(1,0,0)$. The isotropy of the flow has carefully been checked. For more details see Ref. [6].

To concentrate on the dependence on one variable scale, we calculated the ratios

under λ as λ^{ξ_n} , thus avoiding any prejudice in the factorization about multiscaling or not multiscaling.

An alternative derivation of Eq. (5) is given in Ref. [7], based on the multifractal view of the turbulent cascade. It does not explicitly make use of the Navier-Stokes equation. That approach can even account for higher order corrections to the prediction (5), see below.

The importance of verifying the factorization (‘‘fusion rule’’) (5) is evident. We do this here by applying it to the $J_n(r,R)$ of Eq. (2). Decompose at first $v^{n-1}(R)$ in Eq. (2) into $[u(x+R) - u(x)]v^{n-2}(R)$. Then, next, respect $u(x \pm r)u(x+R)$ and thus also $u(x)u(x+R)$ to have correlation 0 as the consequence of the statistical independence of the velocities at two widely separated positions $\mathbf{x} + \mathbf{r}$, $\mathbf{x} + \mathbf{R}$ because $r \ll R$. These correlations are even supposed to vanish if the additional factor $v^{n-2}(R)$ is included. Thus we are left with

$$J_n(r,R)/J_2(r,R) = (C_n/C_2) S_n(R)/S_2(R), \quad (8)$$

displayed in Figs. 1 and 2 for $n=4$ and 6, respectively. For these plots we have divided the LHS of Eq. (8) by the expected scaling behavior $S_n(R)/S_2(R)$. Therefore, if Eq. (8) holds, one would have a straight line. Indeed, for the ISR scales $r=18\eta$ and $r=36\eta$ where Eq. (8) is supposed to hold, we see such behavior, see the upper curves in Figs. 1 and 2.

The derivation of Benzi *et al.* [7] of the fusion rules, which is only based on the assumption of an uncorrelated multiplicative process for the energy cascade, is able to even give the correction term in Eq. (8). We will show this explic-

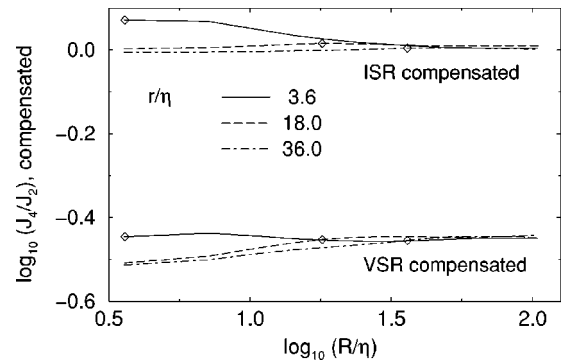


FIG. 1. The upper curves are (in a double logarithmic plot) $J_4(r,R)J_2^{-1}(r,R)/S_4(R)S_2^{-1}(R)$ versus R/η . Here η is $(\nu^3/\epsilon)^{1/4}$ and $\epsilon=1$ in our units. From top to bottom $r/\eta=3.6, 18,$ and 36 , thus from VSR to ISR. The symbols \diamond indicate that here $r=R$, i.e., only at the right of \diamond the assumption $r \ll R$ can be considered as (at least approximately) fulfilled. The lower triple of curves shows the analogous information if $J_4(r,R)J_2^{-1}(r,R)/S_5(R)S_3^{-1}(R)$ is plotted on the ordinate, i.e., compensation with the VSR fusion rule (15) is chosen. The inertial range starts at $R/\eta = \mathcal{O}(10)$.

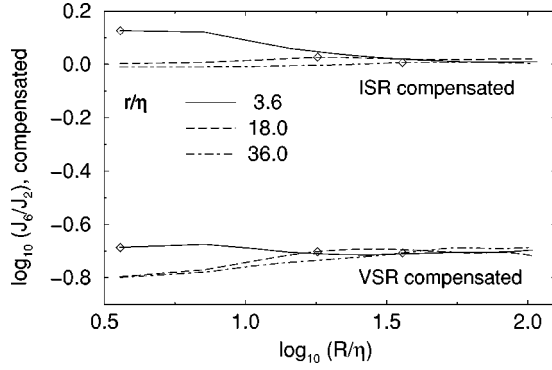


FIG. 2. The corresponding results for $n=6$ as in Fig. 1 for the case $n=4$. $J_6(r,R)J_2^{-1}(r,R)$ is divided by the ISR fusion rule prediction $S_6(R)S_2^{-1}(R)$ in the upper triple of curves and by the VSR fusion rule prediction $S_7(R)S_3^{-1}(R)$ in the lower triple. Again $r < R$ holds on the right of the symbols \diamond . The VSR-ISR transition is at $R/\eta = \mathcal{O}(10)$.

itly for the case of $J_4(r,R)$: Following Ref. [7] and applying the so called ‘‘Ward identity,’’ we first get the exact relation

$$S_4(R-r) = S_4(R) + S_4(r) - 4\tilde{\mathcal{F}}_{1,3}(r,R) - 4\tilde{\mathcal{F}}_{3,1}(r,R) + 6\tilde{\mathcal{F}}_{2,2}(r,R). \quad (9)$$

In the limit of $r/R \rightarrow 0$ such that $S_4(R-r) \approx S_4(R)(1 - \zeta_r r/R)$ and with Eq. (10) of Ref. [7] for $\tilde{\mathcal{F}}_{3,1} = \tilde{\mathcal{F}}_{1,3}$ (for which the fusion rules erroneously give 0 as elaborated in Ref. [7]) we finally obtain the higher order correction in Eq. (8), namely,

$$\frac{J_4(r,R)}{J_2(r,R)} = \frac{C_4}{C_2} \frac{S_4(R)}{S_2(R)} \left[1 + \mathcal{O}\left(\frac{rS_2(R)}{RS_2(r)}\right) + \mathcal{O}\left(\frac{S_3(r)S_2(R)}{S_3(R)S_2(r)}\right) + \mathcal{O}\left(\frac{S_4(r)S_2(R)}{S_4(R)S_2(r)}\right) \right]. \quad (10)$$

The first two correction terms on the RHS are—up to intermittency corrections—order of $(r/R)^{1/3}$, the last one is order of $(r/R)^{2/3}$. Indeed, qualitatively we see such a correction in Fig. 1, upper, for the $r/\eta = 3.6$ curve: The smaller R , the larger the correction to the plateau. [For the other two curves the condition $r/R \ll 1$ used in the derivation of Eq. (10) is not fulfilled throughout.] Unfortunately, the scaling exponents of the correction terms cannot be extracted due to the short scaling regime.

In order to judge whether the horizontal lines in Figs. 1 and 2 are incidental, we have studied in addition another plausible, alternative factorization formula that might stand instead of Eq. (5). Apparently, r and R have not been treated symmetrically, when factorizing $\mathcal{F}_n(r,R)$. If one argues differently than before that the $n-p$ larger eddies, because they carry the energy, are correlated as if the smaller r eddies were not present, the decomposition $\mathcal{F}_n(r,R) = \mathcal{F}_{n-p}(R)\tilde{\mathcal{F}}_{p,n}(r,R)$ would be natural. As before, statistical independence of the r and R eddies lets one skip the R dependence in $\tilde{\mathcal{F}}_{p,n}$. The conservation of the global scaling $\propto \lambda^{\zeta_n}$ then leads to

$$\tilde{\mathcal{F}}_{p,n}(\lambda r) = \lambda^{\zeta_n - \zeta_{n-p}} \tilde{\mathcal{F}}_{p,n}(r). \quad (11)$$

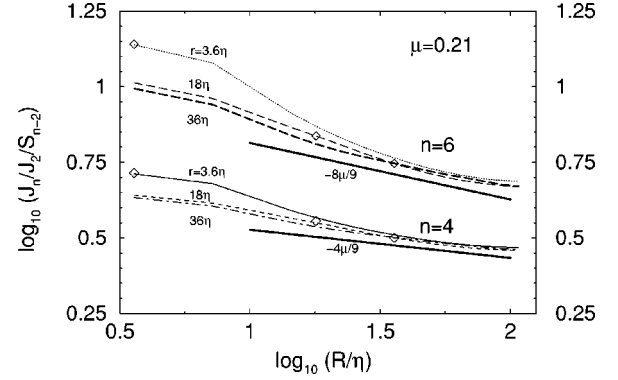


FIG. 3. Compensated plots $J_n J_2^{-1} / S_{n-2}$ as functions of R/η for $n=4$ (lower) and $n=6$ (upper), choosing $r = 3.6\eta$, 18η , and 36η . Again \diamond indicates where $R=r$; the relevant range $r < R$ is towards the right. The full straight lines represent the slopes $-4\mu/9 = -0.093$ and $-8\mu/9 = -0.187$ for $\mu = 0.21$ (taken from [6] as an appropriate fit value in the K62 intermittency model). J_n/J_2 clearly seems to behave as $S_n(R)/S_2(R)$ instead of $S_{n-2}(R)$.

As a consequence scaling-wise we have $\tilde{\mathcal{F}}_{p,n}(r) \propto S_n(r)/S_{n-p}(r)$, altogether the alternative fusion rule

$$\mathcal{F}_n(r,R) \sim S_{n-p}(R)S_n(r)/S_{n-p}(r). \quad (12)$$

In contrast to the original factorization $\sim R^{\zeta_n - \zeta_p}$ this one scales as $R^{\zeta_{n-p}}$, in both cases the global R and r scaling being conserved, $\propto \lambda^{\zeta_n}$. There is no difference in case of monoscaling, while for multiscaling, $\zeta_{n-p} \neq \zeta_n - \zeta_p$, both decompositions differ.

Applying Eq. (12) to J_n of Eq. (6) we find instead of Eq. (7),

$$J_n(r,R) \propto r^{-2} S_n(r) S_{n-2}^{-1}(r) S_{n-2}(R). \quad (13)$$

Accordingly

$$J_n(r,R)/J_2(r,R) = \hat{C}_n(r) S_{n-2}(R), \quad (14)$$

with $\hat{C}_n(r) \propto S_n(r)/[S_2(r)S_{n-2}(r)]$, since $S_0(R) = S_0(r) = 1$. Figure 3 presents compensated plots according to this alternative ISR fusion rule. Apparently, the original fusion rules Eq. (5) and (8), respectively, are superior, the alternatives (12) and (14) can be discarded.

One can understand the different slopes in Fig. 3 relative to Figs. 1,2 (upper) even quantitatively. The difference of the slopes for the two ISR fusion rules is $\delta_n = \zeta_n - \zeta_2 - \zeta_{n-2}$. It fully indicates multiscaling, because $\delta_n = 0$ in the monoscaling case K41. For simplicity we consider the multiscaling model K62 (see Refs. [8,9]) $\zeta_n = n/3 - \mu n(n-3)/18$ and find $\delta_n = -(2\mu/9)(n-2)$. In particular $\delta_2 = 0$, $\delta_4 = -4\mu/9$, and $\delta_6 = -8\mu/9$. These slopes are marked in Fig. 3 and seem to be consistent with the empirical slopes in the compensated curves of the alternative fusion rule. Given the small Reynolds number, one can of course argue whether there is scaling at all.

We conclude that the scaling of the $n-p$ large R eddies is well affected by the presence of the p smaller r eddies, this effect being due completely to multiscaling. In contrast, the small r eddies are curling as if they were free, unaffected by the large eddies in whose field they move.

The factorization rule (7) for the choice $\eta_n \ll r \ll R$ has been confirmed previously already with measured data [10]. [In Ref. [10] the J_n erroneously have an additional factor $n/2$; for the structure functions the $S_n^*(R)$ are used.] Due to restrictions in the small r resolution of the measured data, a verification of the VSR fusion rules was not possible. This was another motivation for the present numerical work.

We now consider the easily accessible case when r is in the VSR, i.e., $r/\eta < \mathcal{O}(10)$. The argument for the factorization (5) was based on strictly keeping the scaling exponent ζ_n of \mathcal{F}_n also in its factorized form. We tacitly assumed that the small r as well as the large R scaling exponents are the ISR type ζ_p , which is natural if both small r and large R are in the ISR. If $r \in$ VSR, its scaling exponent ζ_p is regular, instead, $\zeta_p \rightarrow p$. Then the homogeneity exponent of $\tilde{\mathcal{F}}_{p,n-p}(R)$ under rescaling with λ is ζ_{n-p} instead of $\zeta_n - \zeta_p$. Therefore $\tilde{\mathcal{F}}_{p,n-p}(R)$ can no longer be described by the ratio $S_n(R)/S_p(R)$ because R is in the ISR and thus the denominator has the scaling behavior ζ_p , but not p as desired. Therefore the ISR factorization rule (7) is expected to become invalid if r is below $\approx 10\eta$. This is supported by Figs. 1 and 2 (lower).

Incidentally, if both r and R are in the VSR they both have regular monoscaling exponents p and $n-p$. But here the argument of statistical independence due to $r \ll R$ ceases to be valid, i.e., no factorization is possible anymore; and it is not necessary either, because there is regular r, R dependence.

If $r \ll \eta_n \ll R \ll L$, denoted as the (r)VSR case, two competing factorizations are at hand. One of them is derived in Refs. [2] and [1], saying

$$J_n(r, R) = \tilde{C}_n S_{n+1}(R) / S_3(R). \quad (15)$$

The other one, which strictly adheres to the invariance of the total \mathcal{F}_n scaling behavior under factorization reads

$$J_n(r, R) = \hat{C}_n \frac{S_2(r)}{r^2} \frac{S_n(R)}{R^2} \sim \frac{S_2(r)}{r^2} \frac{S_n(R)}{S_3^2(R)},$$

$$r \in \text{VSR}, R \in \text{ISR}, r \ll R. \quad (16)$$

This factorization is based on the assumption that the n th order correlation has the homogeneity exponent ζ_n irrespective of r, R being in the same or in different subranges. The RHS has scaling exponent ζ_n , because $S_2(\lambda r) \propto \lambda^2 S_2(r)$ for $r \in$ VSR and also $S_3^2(\lambda R) = \lambda^2 S_3^2(R)$ for $R \in$ ISR, since $S_3 \propto R$ from the Howard–van Kármán–Kolmogorov structure equation. [More generally $\mathcal{F}_n(r, R) \propto S_p(r) S_n(R) / S_3^p(R)$.]

There is not much difference between Eqs. (15) and (16) in the small r dependence, because $S_2(r) \propto r^2$ for small r . The factorization (15) says that the LHS is independent of r once r is less than η . It furthermore states that the $n-2$ factors of $v(R)$ in J_n scale with exponent $\zeta_{n+1} - 1$ or, if

$$J_n(\lambda r, \lambda R) = \lambda^{\tilde{\zeta}_n} J_n(r, R) \text{ then } \tilde{\zeta}_n = \zeta_{n+1} - 1. \quad (17)$$

Since in the equation of motion the $r \rightarrow 0$ limit of $J_n(r, R)$ is needed, the VSR factorization (“fusion”) rule is of considerable importance. The quality of Eq. (15) for numerical turbulence is tested in Figs. 1 and 2, lower triples respectively.

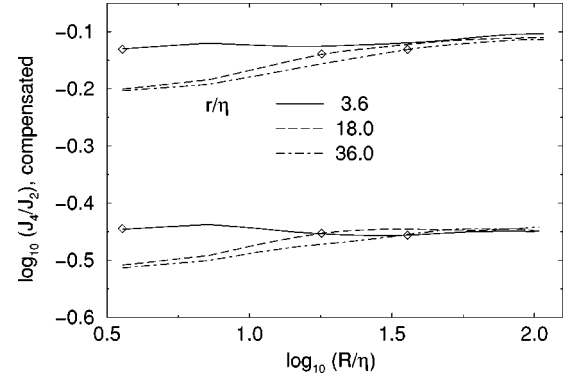


FIG. 4. The VSR factorization (15), i.e., $J_4 J_2^{-1}$ divided by $S_5^* S_3^{-1}$ (upper triple) or by $S_5 S_3^{-1}$ (lower triple). The latter is the same as in Fig. 1. For more information see the caption of Fig. 1. While the two triples of curves are structurally similar, there are differences in detail if the S_n^* or the S_n are taken.

Again, we use compensated plots, this time dividing J_n/J_2 by the expected VSR-scaling behavior, i.e., the right hand side of Eq. (15). If that holds, one would again expect a straight line. Indeed, if $r = 3.6\eta$, i.e., r is in the VSR, the line is straighter than for r values in the ISR, but the result is not completely conclusive because of the low Reynolds number.

We also present Figs. 4 and 5 in order to identify possible differences if S_n^* is taken instead of S_n . This is irrelevant in the case of the inertial range factorization rule, since the involved $n = 2, 4, 6$ are all even. But the VSR factorization (15) comprises odd n . As Figs. 4 and 5 show there are noticeable differences in the details of the respective upper and lower triples, but the curves are structurally the same.

An argument leading to Eq. (15) is start with the ISR fusion rule (7) and reduce r continuously to submerge in the VSR eventually. That means, keep the R dependence of the RHS and fix r at the crossover from the ISR to the VSR, i.e., fix r at $\mathcal{O}(\eta_n)$. Then $r^{-2} S_2(r) \propto \eta_n^{-2} \eta_n^{\zeta_2}$. Now it is important that the crossover scale η_n not only depends on the order n of the moment but also on the scale R , see [1], according to

$$\eta_n = \eta(R/L)^{x_n},$$

with

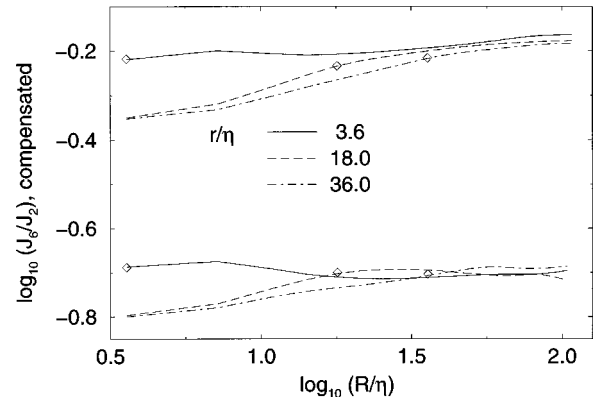


FIG. 5. The VSR factorization (15) of $J_6 J_2^{-1}$ divided by $S_7^* S_3^{-1}$ (upper triple) or by $S_7 S_3^{-1}$ (lower triple). Again there are differences in the detailed behaviors between upper and lower.

$$x_n = (\zeta_n + \zeta_3 - \zeta_{n+1} - \zeta_2)/(2 - \zeta_2). \quad (18)$$

In particular, $\eta_2 = \eta$ as it should. The R dependence of the η_n as well as their n dependence originates from multiscaling as the signature of intermittency. In K41 one has $x_n = 0$ and $\eta_n = \eta$ for all n . Relation (18) implies

$$r^2 S_2(r)|_{r \approx \eta_n} \propto R^{\zeta_{n+1} + \zeta_2 - \zeta_n - \zeta_3}, \quad (19)$$

which when used together with Eq. (7) leads to

$$J_n(r \approx \eta, R) \propto R^{\zeta_{n+1} - \zeta_3}. \quad (20)$$

This is just Eq. (15). For monoscaling (linear n dependence) this coincides with Eq. (7) at $r = \eta$. It therefore is of high interest to identify the validity and the differences between Eqs. (7) and (15), the fusion rules in the r -ISR and r -VSR cases, with convincing significance.

Both r -VSR factorization rules (15) and (16) might not be considered as based on safe arguments. It therefore seems adequate to study the special case $n=2$ separately, where everything can be evaluated explicitly. Only the statistical spatial homogeneity of the flow is used. Start with Eq. (2), choose $n=2$ and find $r^2 J_2(r, R) = \langle u(\mathbf{x} + \mathbf{r})u(\mathbf{x} + \mathbf{R}) - 2u(\mathbf{x})u(\mathbf{x} + \mathbf{R}) + u(\mathbf{x} - \mathbf{r})u(\mathbf{x} + \mathbf{R}) - u(\mathbf{x} + \mathbf{r})u(\mathbf{x}) + 2u^2(\mathbf{x}) - u(\mathbf{x} - \mathbf{r})u(\mathbf{x}) \rangle$. Employing translational invariance, e.g., $u(\mathbf{x} + \mathbf{r})u(\mathbf{x} + \mathbf{R}) \hat{=} u(\mathbf{x})u(\mathbf{x} + \mathbf{R} - \mathbf{r})$, etc., straightforwardly leads to the relation

$$J_2(r, R) = r^{-2} \left\{ S_2(r) + \left[S_2(R) - \frac{1}{2}(S_2(R+r) + S_2(R-r)) \right] \right\}. \quad (21)$$

In the limit $r \rightarrow 0$ one can expand $S_2(r)$ and $[\dots]$ up to second order in r and finds

$$J_2(r, R) = \langle (\partial_1 u_1)^2 \rangle - \frac{1}{2} \frac{d^2 S_2}{dR^2}. \quad (22)$$

If R is in the ISR, the second term becomes small as $R^{\zeta_2 - 2}$, i.e., roughly $\propto R^{-4/3}$, and the first, constant term remains. This is compatible with Eq. (15) for $n=2$, if $\hat{C}_2 = \langle (\partial_1 u_1)^2 \rangle$, while Eq. (16) is excluded because it approaches 0 as $\propto R^{-4/3}$. Also the ISR fusion rule (7) for $n=2$ is reproduced to leading order. On the other hand, the functional dependence of $J_2(r, R)$ on both r and R does not change if r passes from the ISR to the VSR. The only relevant property is $r \ll R$.

A generalization of Eq. (22) for $n > 2$ has been derived in Ref. [7].

$$J_n(r \rightarrow 0, R) = \hat{C}_n \langle (\partial_1 u_1)^2 \rangle \frac{S_n(R)}{S_2(R)} - \frac{1}{n} \frac{d^2}{dR^2} S_n(R), \quad R \in \text{ISR}. \quad (23)$$

If n is large enough, the second term does no longer decrease with increasing R . It grows instead. But still its size shrinks relative to the first term as $R^{\zeta_2 - 2} \rightarrow 0$. For $n=2$ Eq. (22) is recovered. Note that the generalization (23), for large enough

R to neglect the second term, well reproduces the r -ISR fusion rule (7) but does not coincide with the r -VSR rule (15) as it should, since $r \rightarrow 0$ is considered.

To analyze the differences between the ISR and the VSR factorization rules further we now consider the average (discretized) curvature $\Delta_r u$ under the condition that the R -eddy velocity difference $v(x, R; t)$ has the value v_R . We denote this conditional average as $\langle \Delta_r u | v_R \rangle$. It allows us to compute the $J_n(r, R)$ from (2) by using the v_R -probability densities,

$$J_n(r, R) = \int \langle \Delta_r u | v_R \rangle v_R^{n-1} P_R(v_R) dv_R. \quad (24)$$

Here $P_R(v_R)$ is the (unconditioned) probability density to find the R -eddy velocity difference v_R , which can be obtained directly from the numerical solution for each chosen eddy size R , on which P_R depends.

The conditional averages $\langle \Delta_r u | v_R \rangle$ can be calculated via unconditioned probabilities. It is

$$\langle \Delta_r u | v_R \rangle = \int P_{r,R}(\kappa | v_R) \kappa d\kappa = \int \frac{P_{r,R}(\kappa, v_R)}{P_R(v_R)} \kappa d\kappa. \quad (25)$$

Here $P_{r,R}(\kappa, v_R)$ is the common joint probability density to find the field curvature $\kappa \hat{=} \Delta_r u$ and the R -eddy velocity v_R . The fraction has the meaning of the conditional probability $P_{r,R}(\kappa | v_R)$.

The fusion rules (7) and (15) follow immediately if the conditional curvature averages have linear or quadratic dependence on the conditioning eddy field v_R , as was indicated in Refs. [1,10]. In the r -ISR case $\eta \ll r \ll R$ the linear ansatz

$$\begin{aligned} \langle \Delta_r u | v_R \rangle &= [C_n r^{-2} S_2(r) / S_2(R)] v_R \\ &= [J_2(r, R) / S_2(R)] v_R \end{aligned} \quad (26)$$

inserted into Eq. (24) immediately leads to Eq. (7). The quadratic v_R dependence

$$\langle \Delta_r u | v_R \rangle = [\tilde{C}_n / S_3(R)] v_R^2 \quad (27)$$

in turn gives the r -VSR factorization (15). To be more precise, the ansatz (27) is a sufficient condition to imply Eq. (15). Alternatively, as argued in Ref. [11], $\langle \Delta_r u | v_R \rangle$ may be an infinite series in v_R , of which we shall study the beginning, see Eq. (28). The dependencies (26) and (27) on v_R are so markedly different that the conditional average representation (24) seems qualified to become a sensitive check. If Eqs. (26) and (27) could be proven to hold, the validity of the fusion rules (7) and (15) in the r -ISR and the r -VSR cases were strongly supported.

We have determined the conditional averages $\langle \Delta_r u | v_R \rangle$ numerically via $P_{r,R}(\kappa, v_R)$ and $P_R(v_R)$ from Eq. (25) for two values of r , one in the ISR, $r = 36\eta$, the other one in the VSR, $r = 3.6\eta$, as functions of v_R for various fixed R . The curves are displayed in Figs. 6 and 7.

While the linear dependence of $\langle \Delta_r u | v_R \rangle$ nicely confirms the ISR fusion rule (7), the completely missing quadratic v_R dependence (27) excludes the possibility to understand Eq. (15) from a simple product ansatz for the conditional prob-

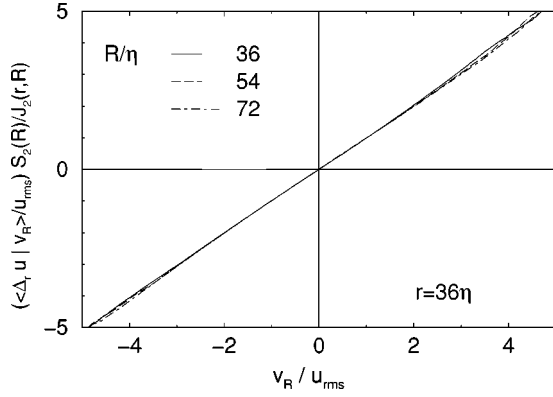


FIG. 6. The conditional average $\langle \Delta_r u | v_R \rangle$ in multiples of $J_2(r, R)/S_2(R)$ versus v_R in multiples of u_{rms} ($= 1.40$) in a double logarithmic plot. $r=36\eta$ is in the ISR. The large eddy scale R varies through $36\eta, 54\eta, 72\eta$, all in the ISR or even in the stirring subrange. The expected linear behavior (26) is evident. The slope of the linear part is 1, as it should.

ability $\langle \Delta_r u | v_R \rangle$, leaving the possibility of an infinite series expansion as stated in Ref. [11] to be tested. The alternative (16), on the other hand, is consistent, $J_n \propto S_n(R)$. Linear laws for the conditional averages have been discussed also in the context of passive scalar advection [11–15]. For the choice $r \in \text{ISR}$ this linear v_R dependence has been studied for Navier-Stokes turbulence by Fairhall *et al.* [10]. In the present paper we add data on r -VSR conditional averages.

We can check the direct method (2) to calculate the J_n and the conditional average representation (24) against each other, see Figs. 8 and 9 for the cases $n=2$ and 3. We have also evaluated J_4 and J_6 and have found similar agreement between the various methods [Eqs. (2) or (24)] as in the case J_2 . The corresponding curves are not displayed here.

To a good approximation the conditional average of the field curvature $\Delta_r u$ depends linearly on v_R , irrespective of r being in the ISR or in the VSR, above or below η . This agrees nicely with the observation in Eq. (21) that η is not explicitly relevant quantity for $J_2(r, R)$.

To control the deviations from the linear behavior we fit-

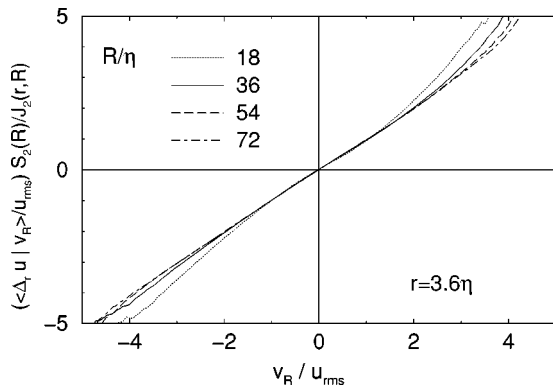


FIG. 7. The conditional average $\langle \Delta_r u | v_R \rangle$ if $r=3.6\eta$ is in the VSR; the same values of R as in Fig. 5. With convincing evidence it is *not* quadratic with respect to v_R but linear, too, at least for negative v_R and up to $\approx 3u_{\text{rms}}$ for positive ones. u_{rms} , by the way, is 1.40. We believe, this asymmetry is a consequence of insufficient statistics for the large fluctuations $|v_R|$ and has not necessarily significance.

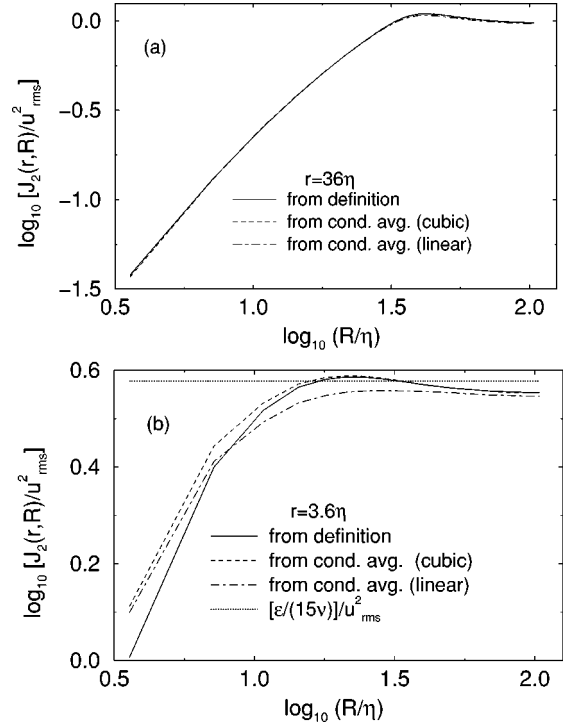


FIG. 8. (a) Double logarithmic plot of $J_2(r, R)$ versus R/η for $r=36\eta$ in the ISR. The directly calculated J_2 from the definition (2) and that from the conditional average representation (24) very well agree, for both the linear and the linear plus cubic interpolation (28) of $\langle \Delta_r u | v_R \rangle$. (b) $J_2(r, R)$ versus R/η if $r=3.6\eta$ is in the VSR. We can compare with the constant value of $\langle (\partial_1 u_1)^2 \rangle$, the dotted horizontal line, as given by Eq. (22). Here the mutual agreement is not very satisfactory. $r=3.6\eta$ might still not be in the asymptotic range $r \rightarrow 0$.

ted the conditional averages with the beginning of a series in v_R ,

$$\langle \Delta_r u | v_R \rangle = f_1(r, R)v_R + f_3(r, R)v_R^3. \quad (28)$$

No even power in v_R is present, because the numerically obtained dependence of the conditional average on v_R is clearly uneven. Inserting Eq. (28) into Eq. (24) leads to

$$J_n(r, R) = f_1(r, R)S_n(R) + f_3(r, R)S_{n+2}(R). \quad (29)$$

If both r and R are in the ISR, the second term is small, see Fig. 6 and Table I, and the ISR factorization (7) obtained. If $r \in \text{VSR}$ the linear and linear plus cubic interpolations differ from each other and also from J_2 from the definition (2), see Figs. 8 and 9. Table I offers numbers for $f_1(r, R)$ and $f_3(r, R)$.

The series expansion of J_n according to the numerical findings and to the odd power expansion of the conditional averages differs in its symmetry under reflection of the eddy velocity, $v(R) \rightarrow -v(R)$, from the VSR fusion rule (15). It behaves as $(-1)^n$, while Eq. (15) goes as $(-1)^{n+1}$. It thus is not yet clear, how the VSR rule $J_n \sim S_{n+1}(R)/R$ can be reconciled with the conditional average results. Further analysis is clearly necessary to get a sufficiently firm base for the r -VSR fusion properties.

If the flow field curvature $\Delta_r u$ is not discretized the resulting correlation function has some resemblance to

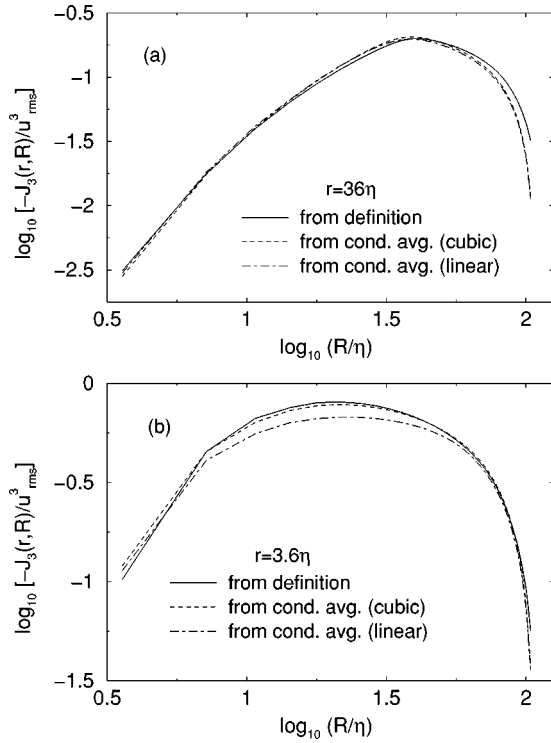


FIG. 9. $-J_3(r,R)$ versus R/η for the two cases $r=36\eta$ (a) and $r=3.6\eta$ (b). With the cubic fit for the conditional average there is good agreement between the direct and the conditional average calculations of J_3 . See also Fig. 8.

$\langle \epsilon v^{n-1}(R) \rangle$, where $\epsilon(x,t)$ denotes the local dissipation rate per mass. In Ref. [2] so-called bridge relations for such objects have been advocated, saying here that

$$\langle \epsilon v^{n-1}(R) \rangle \propto S_{n+2}(R)/R. \quad (30)$$

This relation compares with the r -VSR factorization rule (15). But note, ϵ in Eq. (30) contains two factors of u and is a (gradient u)—squared and thus is a different correlation function as J_n . The bridge relation (30) has recently been checked [16] by numerical solution on a 512^3 lattice, Re_λ

TABLE I. Representative values for the coefficients $f_1(r,R)$ and $f_3(r,R)$ of the conditional average interpolation formula (28). Upper: the ISR case $r=36\eta$; lower: the VSR choice $r=3.6\eta$. The cubic term is markedly larger if r is in the VSR.

R/η	36	54	72	
f_1	1.12	0.852	0.702	
f_3/f_1	0.00221	0.00184	0.00166	
R/η	18	36	54	72
f_1	7.90	3.97	3.00	2.58
f_3/f_1	0.0167	0.00685	0.00306	0.00274

$=220$ and 300 , and found to be valid within reasonable approximation in a compensated plot. It seems worthwhile to also study the conditional average representation which as we found may be more sensitive.

To conclude, the ISR factorization or ‘‘fusion’’ rules are shown to be ‘‘valid’’ under various different checks. But we also caution the reader: In Ref. [7] it has been pointed out that in order to have a very clear test of the fusion rule predictions, one has to have $\text{Re}_\lambda \approx 2000$. There is no change in any numerical study to achieve this. However, the benefit of numerical studies can be good resolution towards small scales. We find that the small scale r -VSR fusion rules are far less clear. The corresponding conditional probabilities are objects to study these fusion rules more sensitively. The conditional average field curvature on scale r , $\Delta_r u$, essentially depends linearly on the conditioning eddy velocity fluctuation, irrespective of r less than or beyond η .

It is our pleasure to acknowledge stimulating discussions with A. Fairhall, I. Procaccia, L. Biferale, and F. Toschi. This work was supported by the German-Israeli Foundation (GIF), and by the DFG through Grant No. SFB185-D3. It also is part of the research program of the Stichting voor Fundamenteel Onderzoek der Materie (FOM), which is financially supported by the Nederlandse Organisatie voor Wetenschappelijk Onderzoek (NWO). Computer time was supplied by the NIC in Jülich.

[1] A.L. Fairhall, V.S. L’vov, and I. Procaccia, *Europhys. Lett.* **43**, 277 (1998).
 [2] V.S. L’vov and I. Procaccia, *Phys. Rev. Lett.* **77**, 3541 (1996).
 [3] V.S. L’vov and I. Procaccia, *Phys. Rev. Lett.* **76**, 2898 (1996).
 [4] V.S. L’vov and I. Procaccia, *Phys. Rev. E* **54**, 6268 (1996).
 [5] S. Grossmann, D. Lohse, and A. Reeh, *Phys. Rev. E* **56**, 5473 (1997).
 [6] S. Grossmann, D. Lohse, and A. Reeh, *Phys. Fluids* **9**, 3817 (1997).
 [7] R. Benzi, L. Biferale, and F. Toschi, *Phys. Rev. Lett.* **80**, 3244 (1998); R. Benzi, L. Biferale, G. Ruiz-Chavarria, S. Ciliberto, and F. Toschi, *Phys. Fluids* **11**, 2215 (1999).
 [8] A.N. Kolmogorov, *J. Fluid Mech.* **13**, 82 (1962).

[9] A.M. Obukhov, *J. Fluid Mech.* **13**, 77 (1962).
 [10] A.L. Fairhall, B. Dhruva, V.S. L’vov, I. Procaccia, and K.R. Sreenivasan, *Phys. Rev. Lett.* **79**, 3174 (1997).
 [11] E.S.C. Ching, V.S. L’vov, E. Podivilov, and I. Procaccia, *Phys. Rev. E* **54**, 6364 (1996).
 [12] V. Yakhot and Y. Sinai, *Phys. Rev. Lett.* **63**, 1965 (1991).
 [13] P. Kailasnath, K.R. Sreenivasan, and J.R. Saylor, *Phys. Fluids A* **5**, 3207 (1993).
 [14] R.H. Kraichnan, *Phys. Rev. Lett.* **72**, 1016 (1994).
 [15] A.L. Fairhall, O. Gat, V.S. L’vov, and I. Procaccia, *Phys. Rev. E* **53**, 3518 (1996).
 [16] A. Ceani and D. Biskamp, *Europhys. Lett.* **46**, 332 (1999).